MNRAS 000, 1–18 (2019) Preprint 15 January 2020 Compiled using MNRAS LATEX style file v3.0

Interacting galaxies in the IllustrisTNG simulations – II: Star formation in the post-merger stage.

Maan H. Hani,[1]★† Hayman Gosain,[1,2] Sara L. Ellison,[1] David R. Patton,[3] Paul Torrey[4]

[1] *Department of Physics and Astronomy, University of Victoria, Victoria, British Columbia, V8P 1A1, Canada*
[2] *Department of Physical Sciences, Indian Institute of Science Education and Research Mohali, Manauli, Punjab 140306, India*
[3] *Department of Physics and Astronomy, Trent University, 1600 West Bank Drive, Peterborough, ON K9L 0G2, Canada*
[4] *Department of Astronomy, University of Florida, 211 Bryant Space Sciences Center, Gainesville, FL, USA*

Accepted XXX. Received YYY; in original form ZZZ

ABSTRACT

Galaxy mergers are a major evolutionary transformation whose effects are borne out by a plethora of observations and numerical simulations. However, most previous simulations have used idealised, isolated, binary mergers and there has not been significant progress on studying statistical samples of galaxy mergers in large cosmological simulations. We present a sample of 27,691 post-merger (PM) galaxies ($0 \leq z \leq 1$) identified from IllustrisTNG: a cosmological, large box, magneto-hydrodynamical simulation suite. The PM sample spans a wide range of merger and galaxy properties ($M_\star$, μ, $f_{\rm gas}$). We demonstrate that star forming (SF) PMs exhibit enhanced star formation rates (SFRs) on average by a factor of ~ 2, while the passive PMs show no statistical enhancement. We find that the SFR enhancements: (1) show no dependence on redshift, (2) anti-correlate with the PM's stellar mass, and (3) correlate with the gas fraction of the PM's progenitors. However, SF PMs show stronger enhancements which may indicate other processes being at play (e.g., gas phase, feedback efficiency). Although the SFR enhancement correlates mildly with the merger mass ratio, the more abundant minor mergers ($0.1 \leq \mu < 0.3$) still contribute $\sim 50\%$ of the total SFR enhancement. By tracing the PM sample forward in time, we find that galaxy mergers can drive significant SFR enhancements which decay over ~ 0.5 Gyr independent of the merger mass ratio, although the decay timescale is dependent on the simulation resolution. The strongest merger-driven starburst galaxies evolve to be passive/quenched on faster timescales than their controls.

Key words: galaxies: evolution – galaxies: star formation – galaxies: interactions – methods: numerical

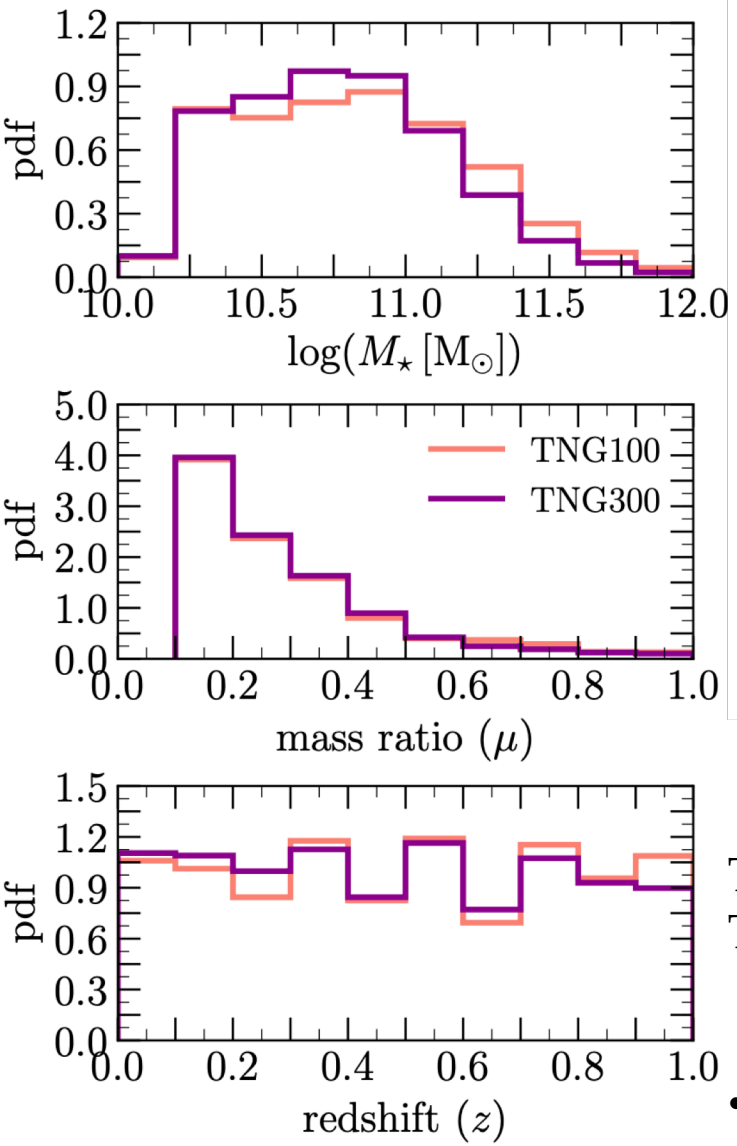

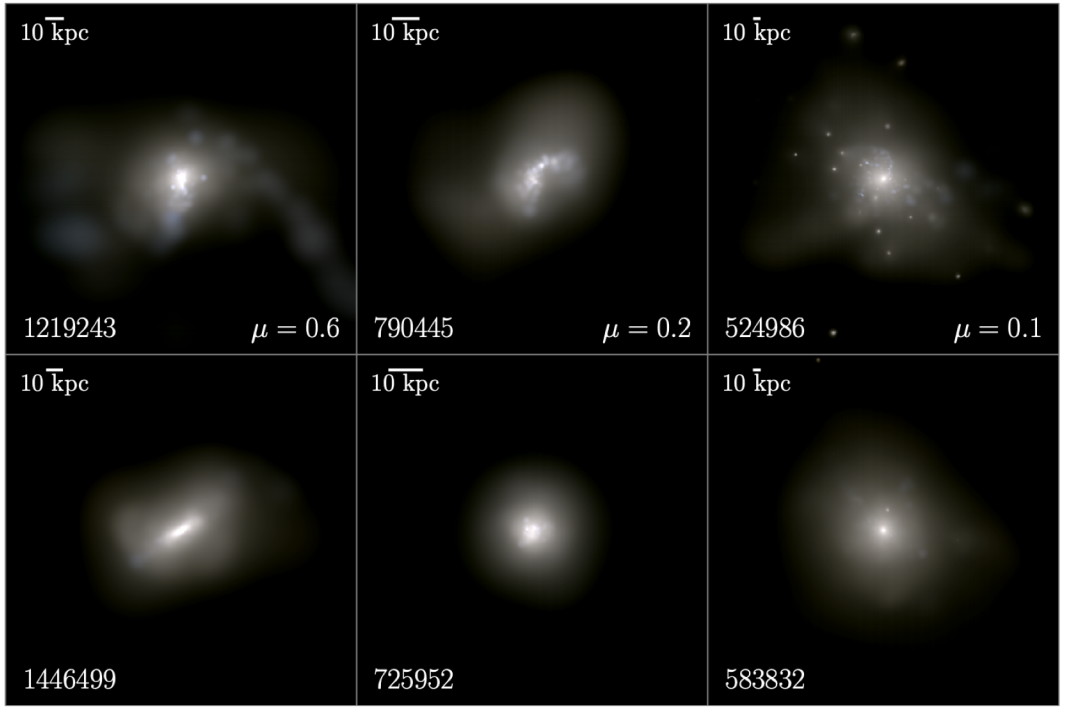

Figure 1. The stellar mass ($M_\star$), mass ratio (μ), and redshift (z) distributions of our post-merger samples selected from TNG100 (salmon histogram) and TNG300 (purple histogram). The sample spans a wide range in mass ratio ($\mu \geq 0.1$) and redshift ($z \leq 1$) which is key when studying the effects of galaxy mergers during the post-merger stage. In total, we selected 1,855 post-mergers from TNG100 and 25,836 from TNG300.

$$10^{10} \leq M_\star/\mathrm{M}_\odot \leq 10^{12},\ z \leq 1$$

TNG100: 1855 пост-мержеров; 263794 контроль
TNG300: 25836 пост-мержеров; 3934409 контроль

Контроль:

- Такое же число галактик N2 в пределах 2 Mpc
- M>10^10 M_sun
- R_sep > 2
- SF: active or passive
- R1 – расстояние от ближайшего компаньона

$$r_{\mathrm{sep}} = \frac{r}{R_{1/2}^{\mathrm{host}} + R_{1/2}^{\mathrm{comp}}}$$

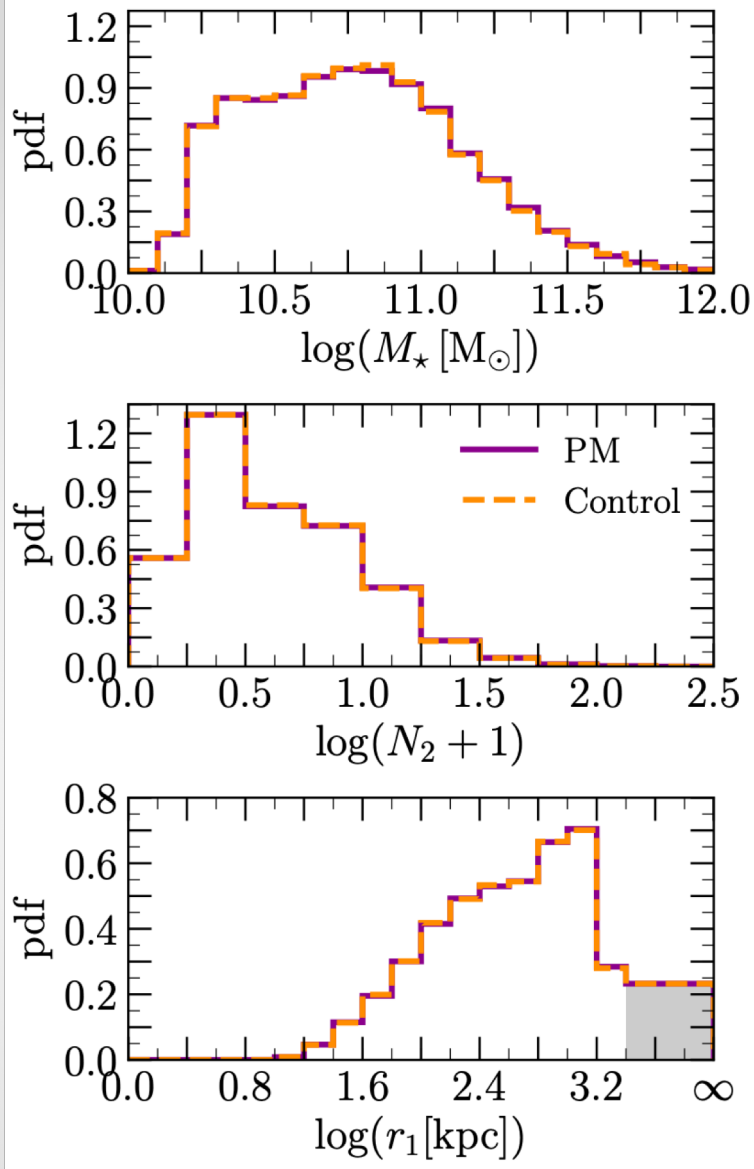

Figure 3. A comparison between the post-merger sample and their respective controls in TNG300-1. The grey shaded bin in the r_1 distribution includes all galaxies with $r_1 > 2$ Mpc. The figure only shows the quantities which are allowed to vary during the control matching (i.e., $M_\star$, N_2, and r_1). The control matching is equally excellent for the TNG100 sample (not shown).

	$Q(sSFR)$	$\sigma_{Q(sSFR)}/\sqrt{N}$
all	2.057	0.024
star-forming	2.073	0.020
passive	0.983	0.022

$$Q(sSFR) \equiv \frac{\langle sSFR_{\rm pm} \rangle}{\langle sSFR_{\rm control} \rangle}$$

TNG100: 1855 пост-мержеров; 263794 контроль
TNG300: 25836 пост-мержеров; 3934409 контроль

Контроль:

- Такое же число галактик N2 в пределах 2 Mpc
- M>10^10 M_sun
- R_sep > 2
- SF: active or passive
- R1 – расстояние от ближайшего компаньона

$$r_{\rm sep} = \frac{r}{R_{1/2}^{\rm host} + R_{1/2}^{\rm comp}}$$

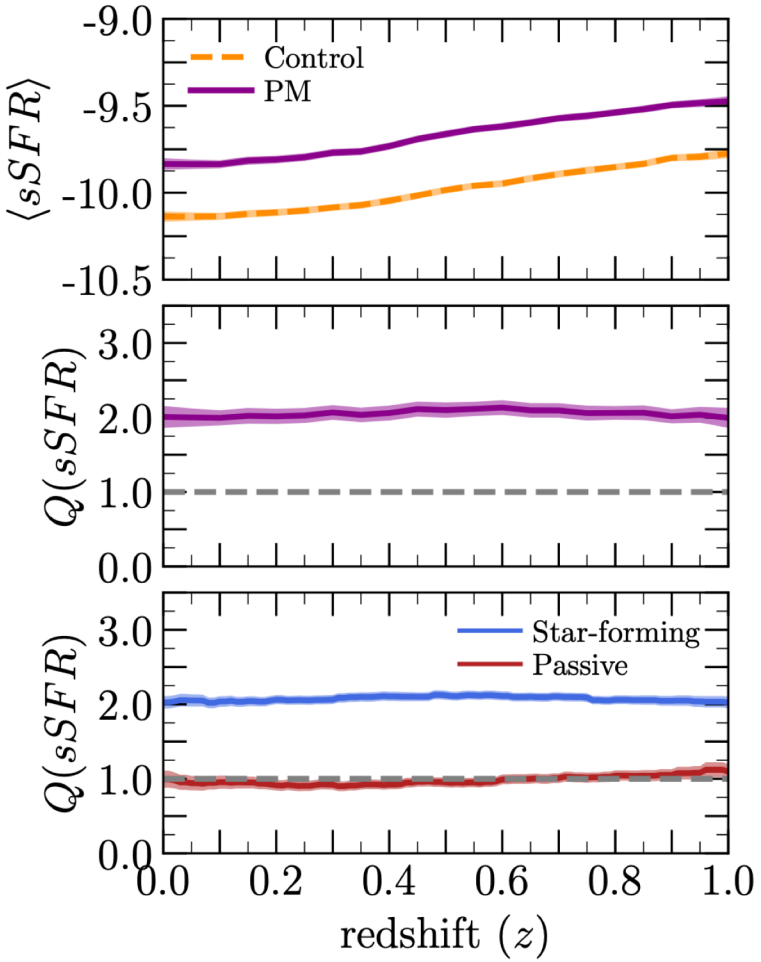

Figure 5. The redshift-evolution of the sSFR enhancement in post-mergers. The top panel shows the running average sSFR for post-mergers (dark-purple) and their associated controls (orange) with the shaded region representing twice the standard error on the mean in bins or redshift. The middle panel shows the dependence of $Q(sSFR)$ (and the associated uncertainty; see equation 2) on redshift for the full post-merger sample while the bottom panel shows $Q(sSFR)$ for star-forming (blue) and passive (red) post-mergers. Post-mergers exhibit enhanced sSFRs at all redshifts ($0 \leq z \leq 1$). The enhancement is dominated by the star-forming post-mergers (67% of the sample) while the sSFRs of passive post-mergers (33% of the sample) are consistent with those of the controls.

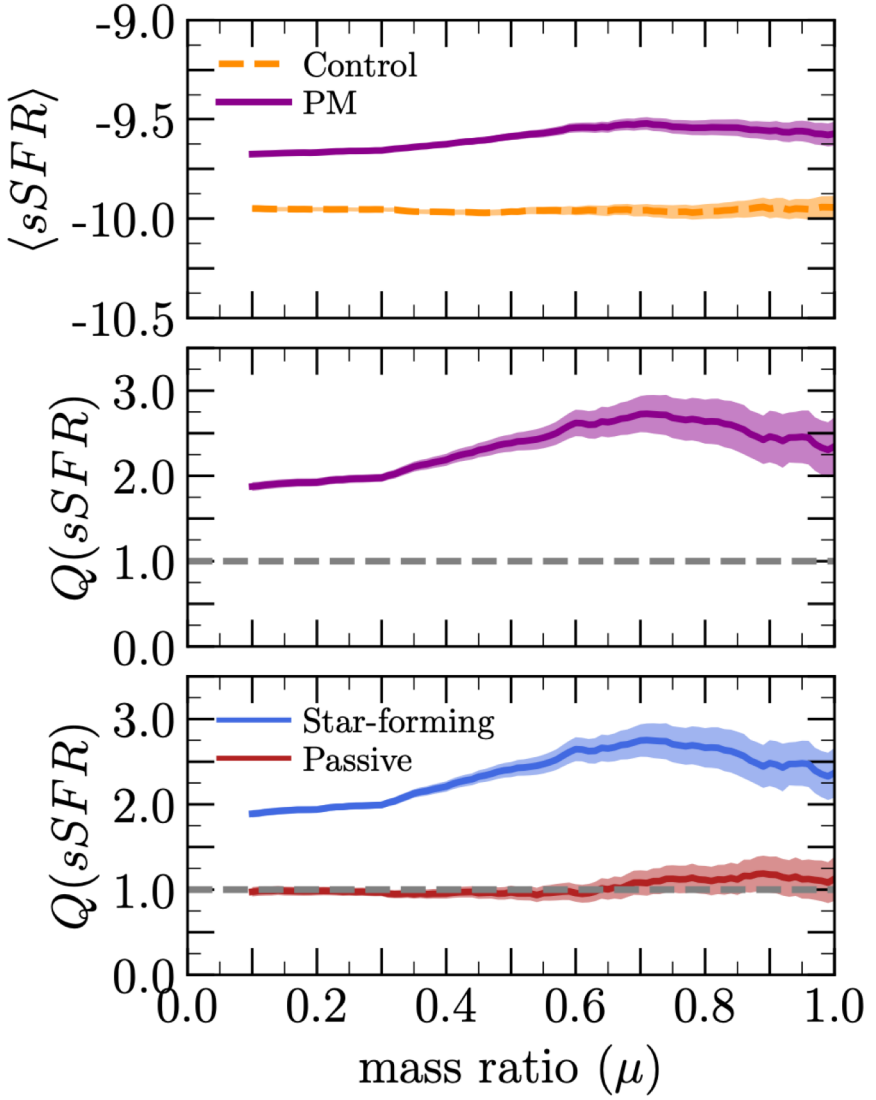

Figure 6. The dependence of the enhancement in the post-mergers' sSFR on the parents' merger mass ratio (μ). The shaded region represents twice the standard error on the mean in bins of μ. Post-mergers exhibit enhanced sSFR for all mass ratios with an increasing enhancement for major mergers. The enhancement is dominated by the star-forming post-mergers, while the passive post-mergers sSFR are consistent with their controls.

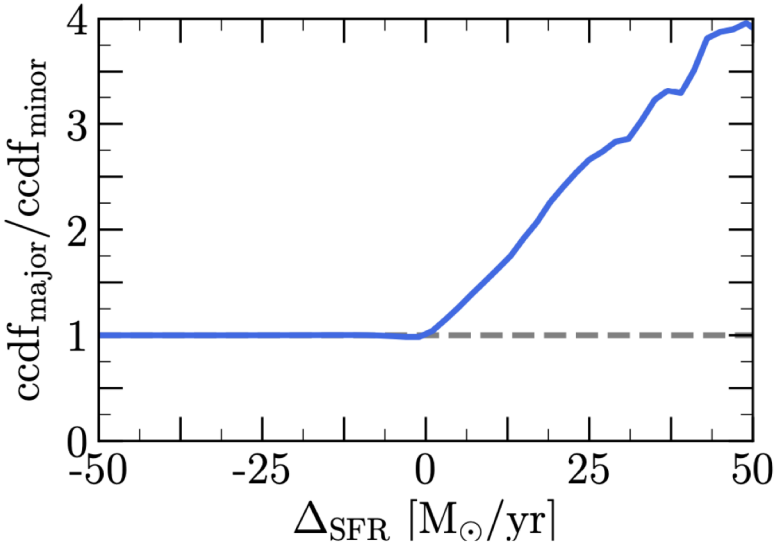

Figure 7. The fraction of star-forming descendants of major mergers ($\mu \geq 0.3$) with SFR enhancement greater than Δ_{SFR} (complementary cumulative distribution function; ccdf) relative to that of minor mergers ($0.1 \leq \mu < 0.3$). The definition of Δ_{SFR} is given in equation 3. Major mergers dominate the high tail of the Δ_{SFR} distribution.

$$\Delta_{\mathrm{SFR}} = SFR_{\mathrm{pm}} - SFR_{\mathrm{SFMS}}.$$

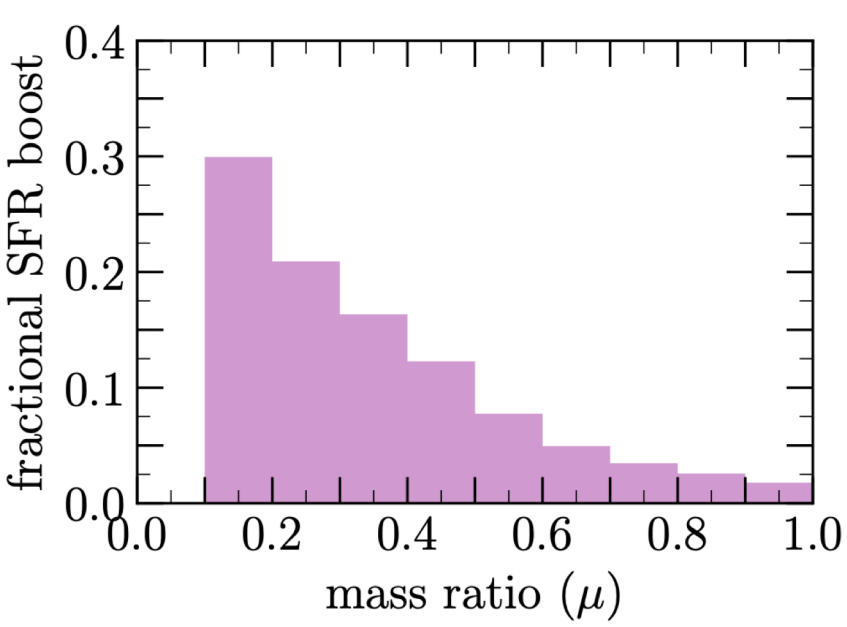

Figure 8. An accounting of the contribution to the total merger-driven SFR enhancement budget in the star-forming post-merger sample. The merger-induced star formation boost for a given post-merger is defined as the vertical offset from the SFMS (see equation 3). The contribution to the total merger-induced SFR enhancement increases with decreasing mass ratio thus indicating that minor mergers ($0.1 \leq \mu < 0.3$) are significant contributors to the global merger-induced SFR budget. Although major mergers ($\mu \geq 0.3$) induce the strongest bursts, the abundance of minor mergers compensates for their modest SFR enhancement when compared to major mergers.

За интенсивные вспышки ЗО ответственность на большом мержинге, но малый мержинг более эффективен в увеличении глобального ЗО

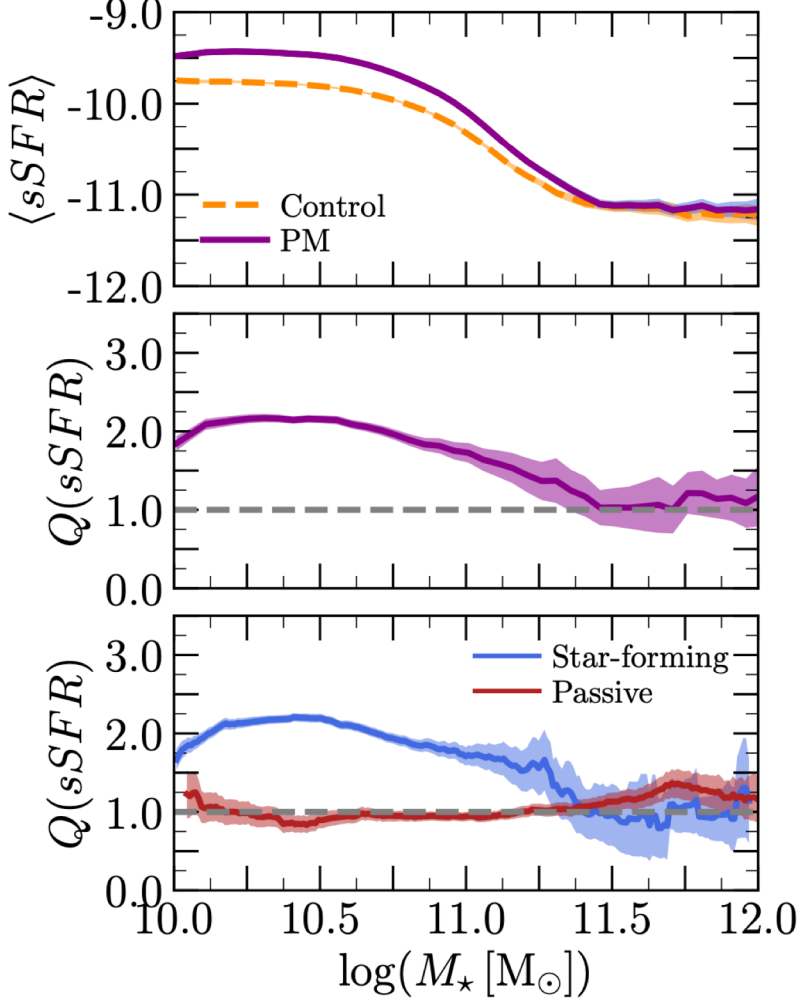

Figure 9. The dependence of the enhancement in the post-merger's sSFR on post-merger stellar mass. The shaded regions represent twice the standard error on the mean in bins of $\log(M_\star/\mathrm{M}_\odot)$. Star formation is most enhanced in post-mergers with $10.0 \leq \log(M_\star/\mathrm{M}_\odot) \leq 11.4$ with a declining enhancement for larger $M_\star$. For $\log(M_\star/\mathrm{M}_\odot) > 11.4$ post-mergers form stars at an average rate which is consistent with that of the control galaxies. The star-forming post-mergers show the same behaviour as the full post-merger sample while passive post-mergers are consistent with no enhancement for all post-merger $M_\star$ with a possible slight enhancement at the largest $M_\star$.

Ожидаемо, наибольший эффект в Q(sSFR) дают галактики со звездообразованием, а не пассивные.

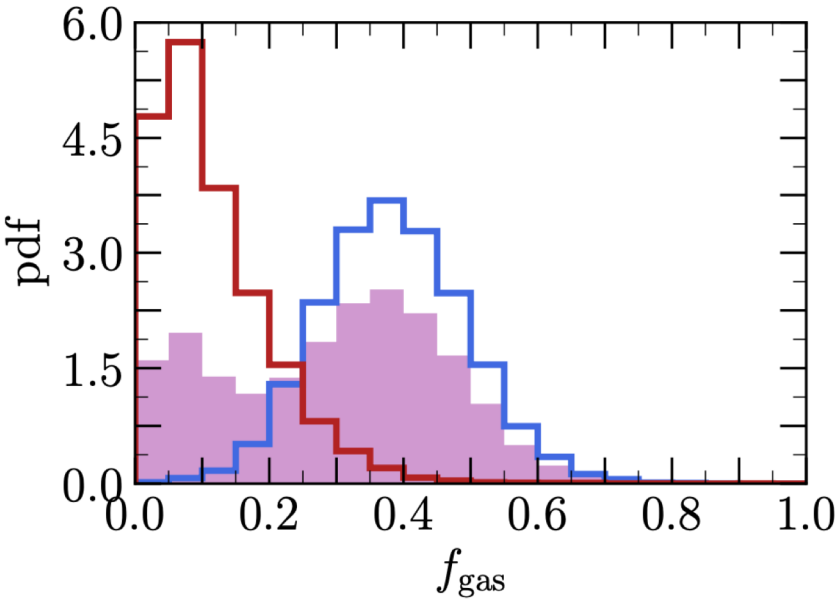

Figure 10. The gas fraction distribution of the post-merger sample in TNG300-1. The filled purple histogram represents the full sample while the red and blue histograms represent the passive and star-forming post-mergers, respectively. The star-forming post-mergers are the descendants of gas-rich mergers when compared to their passive counterparts.

$$f_{\rm gas} \equiv \frac{\sum_{\rm prog} M_{\rm gas}}{\sum_{\rm prog} M_{\rm gas} + \sum_{\rm prog} M_{\star}}$$

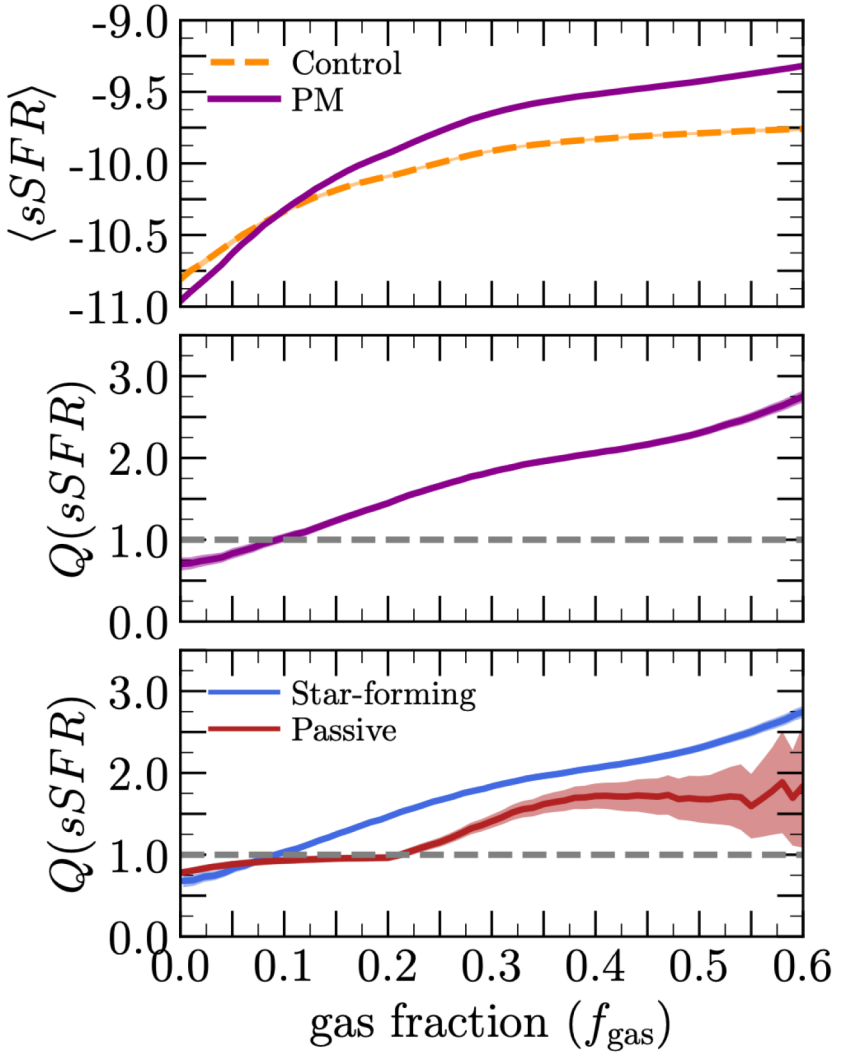

Figure 11. The effect of the progenitors' gas content on the observed enhancement in the post-merger phase. The shaded regions represent twice the error on the mean in bins of $f_{\rm gas}$. Gas rich mergers (i.e., high $f_{\rm gas}$) yield post-mergers with enhanced sSFRs. Alternatively, mergers between gas-poor galaxies (i.e., low $f_{\rm gas}$) develop into post-mergers with suppressed sSFR. The aforementioned correlation between $Q(sSFR)$ and the parents' gas content holds for both star-forming and passive galaxies with the effects being especially pronounced for the star-forming post-merger sample.

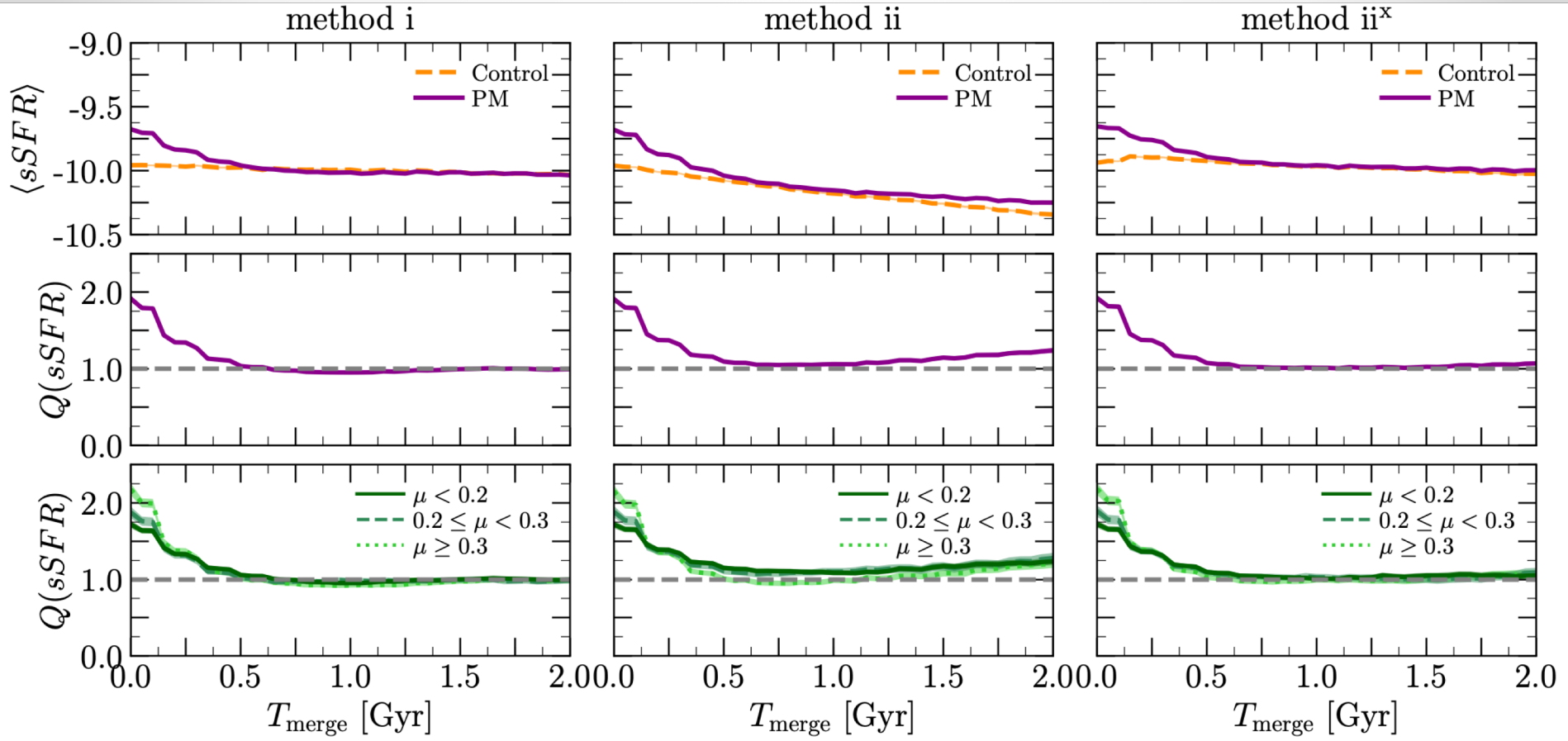

Figure 12. The evolution of star formation during the post-merger phase. The three columns (from left to right) show the results of the tracing/control matching methods: method i, method ii, and method ii^{x}, respectively. The top panels shows the running average sSFR for post-mergers (dark-purple) and their controls (orange) as a function of time after the merger. The middle panels show the evolution of $Q(sSFR)$ for the full post-merger sample, and the bottom panels show $Q(sSFR)$ for a sub-sample of post-mergers selected based on the parents' mass ratios. The shaded regions represent twice the standard error on the mean in bins of $T_{\rm merge}$. All methods show that the enhancement in sSFR decays following the merger and vanishes after $\sim$ 500 Myr. Although mergers with different mass ratios induce enhancements of varying strengths, all enhancements decay similarly after $\sim$ 100 Myr. The enhancement at later $T_{\rm merge}$ shown in method ii (middle column) is driven by the deviation in the post-merger and control properties (namely, different class for post-mergers and controls). Ensuring good control quality (method ii^{x}; right column) removes the spurious enhancements seen at large $T_{\rm merge}$ in method ii.

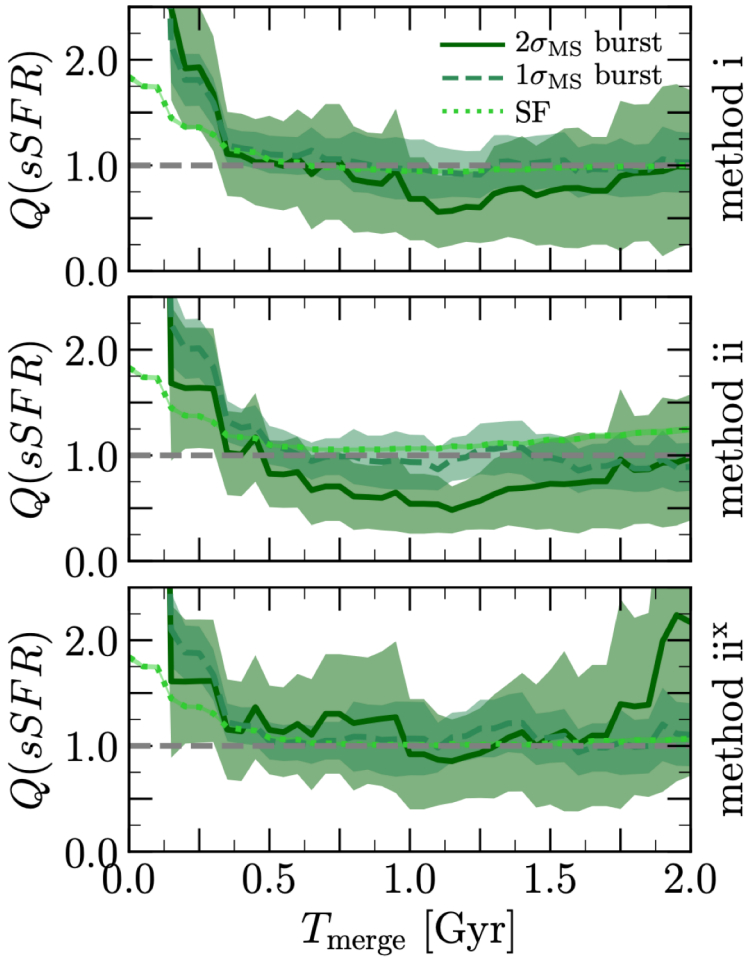

Figure 13. The evolution of star formation during the post-merger phase for post-mergers with different merger-induced starburst strengths. From top to bottom, the panels show $Q(sSFR)$ for a sub-sample of post-mergers selected based on the strength of the SFR at $T_{\rm merge}$ = 0 Gyr and traced using methods i, ii, and ii$^{\rm x}$, respectively. The shaded regions represent twice the standard error on the mean in bins of $T_{\rm merge}$. Independent of the method, the weakest starbursts (i.e., SF, $1\sigma_{\rm MS}$ burst) do not induce suppression in SFR. However, the strongest merger-induced SFRs can evolve to have statistically suppressed star formation. The level and existence of SFR suppression depend on the merger/control tracing method. Note: The $Q(sSFR)$−axis is truncated for visual purposes; 2σ bursts exhibit a peak $Q(sSFR) \simeq 12$ while 1σ bursts

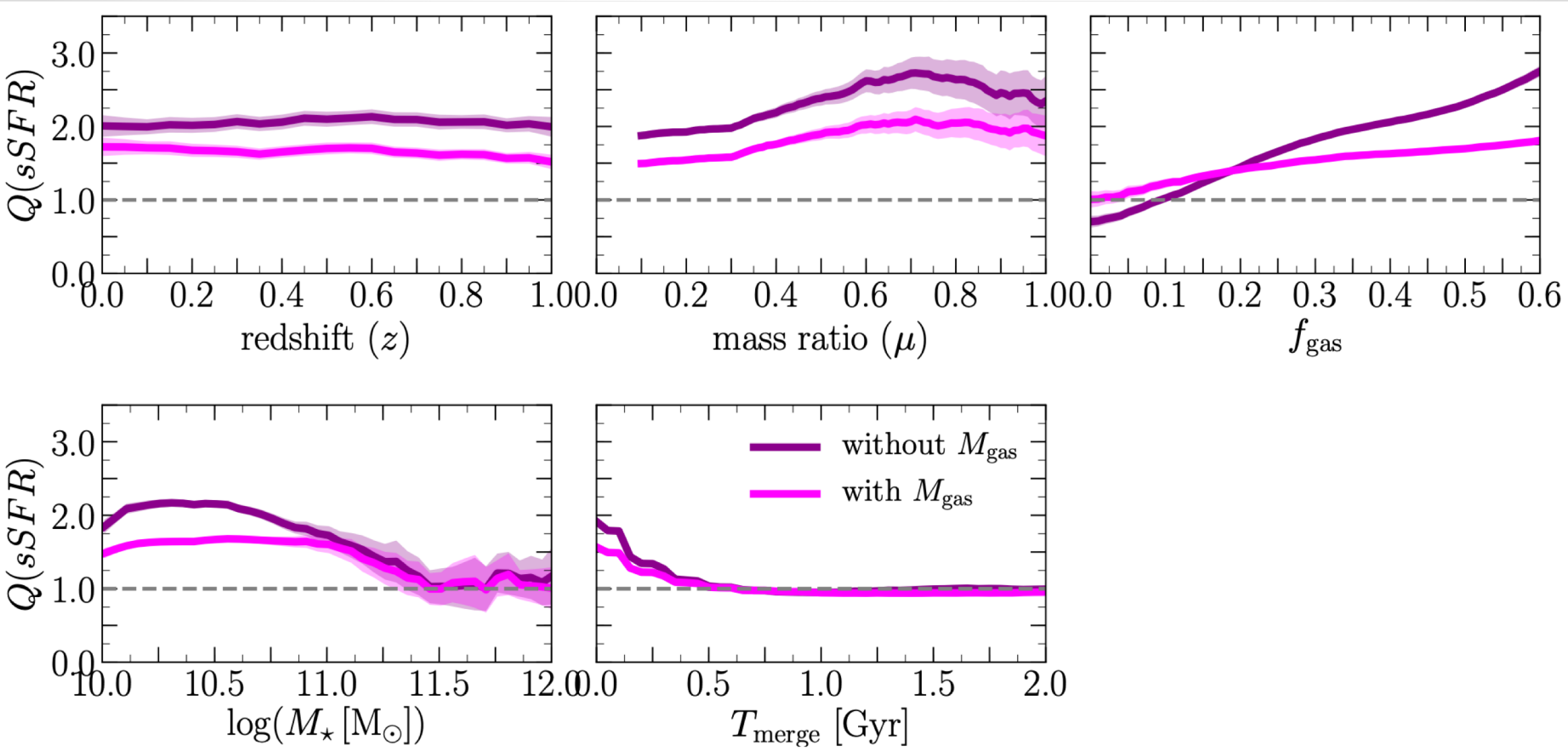

Figure 14. The effect of the controlling for gas mass (i.e., gas fraction) on the measured merger-driven SFR enhancement. The shaded regions represent twice the standard error on the mean. The results of TNG300-1 for two different types of matching, with and without matching on gas mass, are shown in magenta and dark-purple, respectively. Controlling for the gas mass reduces the strength of the measured SFR enhancement (or suppression). Nonetheless the results are consistent between the two control matching techniques.